JASA EXPRESS LETTERS | ARTICLE | asa.scitation.org/journal/jel

Amplitude-invariant phase masking for coherence recovery in scattered wavefields

Akshika Rohatgi,[a] Andrey Bakulin,[b] and Sergey Fomel[c]
Bureau of Economic Geology, University of Texas at Austin, Austin, Texas 78758, USA

Abstract: Coherent summation of multichannel recordings relies on phase stability across measurements. In scattered wavefields, near-surface heterogeneities introduce record-dependent phase distortions that decorrelate otherwise coherent signals and degrade summation quality. Conventional approaches to recovering phase coherence implicitly tie phase estimation to signal amplitude, introducing bias where amplitude variability is large. We present a framework based on circular statistics that separates phase estimation from amplitude entirely, ensuring all records contribute equally to the representative phase regardless of their energy. Synthetic experiments confirm that the proposed method outperforms conventional approaches when amplitude variability is present, offering a practical path toward more robust coherence recovery in seismic imaging and other wave-based sensing applications.

[Editor: Longjun Dong] https://doi.org/10.1121/10.0044229

Received: 18 March 2026 **Accepted:** 12 June 2026 **Published Online:** 1 July 2026

1. Introduction

Phase is a fundamental carrier of information in signals.[1] When phase remains stable across multichannel measurements, coherent summation enhances signal energy through constructive interference.[2] The need to isolate and denoise phase has been recognized across domains ranging from speech processing[3,4] to interferometric synthetic aperture radar deformation mapping.[5] More recently, the same need has been identified in multichannel seismic data, where near-surface scattering introduces strong phase distortions across recorded signals.[6]

In multichannel seismic imaging, signals are broadband and coherence must be evaluated across frequency rather than under single-frequency assumptions. Phase distortions introduced by scattering vary with frequency and receiver position, complicating coherent summation. Beamforming and stacking methods exploit phase alignment across receiver arrays to reinforce coherent arrivals. Recent advances have shown that selectively suppressing incoherent time–frequency components through phase masking can further improve coherence recovery.[7] However, existing masking approaches derive coherence weights from locally stacked or beamformed seismic records, implicitly coupling phase estimation to amplitude information. When amplitudes vary significantly across receivers, this coupling biases the phase estimate and limits coherence recovery precisely where it is most needed.

In this Letter, we introduce an amplitude-invariant phase masking framework grounded in circular statistics. The method decouples phase estimation from amplitude entirely. Building on the work of Bakulin *et al.*,[7] the proposed approach applies a unit-magnitude operator in the complex frequency domain: at each frequency, the phase of each record is replaced with a representative estimate derived from neighboring measurements using the circular mean. We demonstrate that this framework stabilizes phase in scattered wavefields and improves coherence in the presence of both phase perturbations and amplitude variability.

2. Phase distortions in scattered wavefields

When acoustic or elastic waves propagate through media with small-scale heterogeneities, such as rough interfaces or closely spaced sub-wavelength inclusions, cumulative multiple scattering introduces record-dependent phase distortions while preserving a recognizable ballistic arrival. We consider scalar (acoustic, longitudinal P-wave) propagation, although the formulation applies to any complex-valued signal regardless of polarization. The synthetic experiments span the 1–80 Hz band typical of land seismic exploration data. The cumulative effect is a frequency-dependent, spatially varying phase perturbation that differs from record to record, decorrelating otherwise coherent recordings.

[a]Corresponding author: akshikarohatgi@utexas.edu
[b]Email: a_bakulin@yahoo.com
[c]Email: sergey.fomel@beg.utexas.edu

Scattering-induced phase randomization is the physical origin of speckle,[8] observed across acoustics, radar, ultrasound, and interferometric remote sensing. In the complex signal domain, speckle manifests as multiplicative noise: the observed field is the product of a coherent signal and a random phasor whose phase becomes randomized under strong scattering. Analogous multiplicative phase distortions have recently been identified in broadband seismic data, where near-surface scattering introduces random, frequency-dependent phase perturbations across recorded signals, manifesting as severe wavelet distortions in time domain.[9]

Conceptually, a clean recording is described by its complex Fourier spectrum, written in standard polar (magnitude-phase) form[10]

$$A_{clean}(\omega) = \left|A_{clean}(\omega)\right| e^{i\theta_{clean}(\omega)}, \tag{1}$$

where ω is angular frequency, $|A_{clean}(\omega)|$ is the spectral magnitude of the undistorted recording, and $\theta_{clean}(\omega)$ is its phase spectrum.

Under scattering, this clean spectrum acquires a record-dependent phase perturbation $\delta_k(\omega)$. The perturbations are statistically independent across both records and frequencies and frequency-dependent in character. The spectral amplitude $\left|A_{clean}(\omega)\right|$ is first kept unchanged; the decorrelation is entirely phase driven.

The perturbed spectrum of the kth recording in a multichannel seismic ensemble can, therefore, be written as

$$A_k(\omega) = \left|A_{clean}(\omega)\right| e^{i\theta_k(\omega)}, \qquad \theta_k(\omega) = \theta_{clean}(\omega) + \delta_k(\omega). \tag{2}$$

Here, k indexes individual recorded traces in the ensemble. In the time domain, this phase perturbation produces distorted waveform shapes [Fig. 1(c)], mimicking scattering-induced phase scrambling observed in field data.

In practice, trace amplitudes also vary due to geometric spreading, attenuation, source coupling, and scattering losses. Incorporating trace-dependent amplitude scaling α_k drawn from a uniform distribution on [0, 1] gives

$$A'_k(\omega) = \alpha_k \left|A_{clean}(\omega)\right| e^{i\theta_k(\omega)}. \tag{3}$$

This two-stage synthetic design separates the experiment into (i) phase-only perturbations with uniform amplitudes [Fig. 1(c)] and (ii) the same phase perturbations combined with record-dependent amplitude scaling [Fig. 1(d)]. The staged construction is essential because, as shown in Sec. 3, the two phase-masking estimators are theoretically equivalent in stage (i) and diverge only in stage (ii). Separating the stages, therefore, isolates the regime in which amplitude bias matters. Therefore, suppressing these perturbations requires an operator that acts exclusively on the phase component of the spectrum.

3. Phase-only coherence conditioning via phase masking

Restoring coherence across a scattered wavefield requires correcting record-dependent phase perturbations. We focus exclusively on phase distortions, which are often not explicitly corrected in conventional seismic signal-processing workflows. Amplitude effects can be addressed separately; here, our goal is to correct phase inconsistencies while preserving the original spectral amplitudes.

A phase mask accomplishes this as a multiplicative, unit-magnitude operator in the complex frequency domain that replaces the phase of each record with a locally estimated representative phase while leaving spectral amplitudes exactly unchanged.[7]

For the record $\boldsymbol{k}$, the phase mask at frequency $\boldsymbol{\omega}$ is defined as

$$PM_k(\omega) = \exp\left(i\left[\hat{\theta}_k(\omega) - \theta_k(\omega)\right]\right). \tag{4}$$

The mask is applied directly to the original complex spectrum, and the masked output is

$$\tilde{\boldsymbol{A}}_{\boldsymbol{k}}(\boldsymbol{\omega}) = \left|\boldsymbol{A}_{\boldsymbol{k}}(\boldsymbol{\omega})\right| e^{i\hat{\boldsymbol{\theta}}_{\boldsymbol{k}}(\boldsymbol{\omega})}, \tag{5}$$

where $\hat{\boldsymbol{\theta}}_{\boldsymbol{k}}(\boldsymbol{\omega})$ is the representative phase estimated from local records that samples comparable propagation paths. By construction $\left|\boldsymbol{PM}_{\boldsymbol{k}}(\boldsymbol{\omega})\right| = 1$ at all frequencies, so spectral energy is preserved and the operator is designed to modify phase only.

The two methods compared next share this information and differ only in how $\hat{\boldsymbol{\theta}}_{\boldsymbol{k}}(\boldsymbol{\omega})$ is estimated from the local ensemble.

3.1 Phase masking via local stacking (PLS)

One approach to estimating the representative phase is to average the ensemble of n recorded seismic signals, $x_k(t)$, in the time domain. The phase of the resulting stack,

$$x_{stack}(t) = \frac{1}{n}\sum_{k=1}^{n} x_k(t), \tag{6}$$

defines $\theta_{stack}(\omega)$ as the phase spectrum of $x_{stack}(t)$, which then serves as the representative phase: $\hat{\theta}_{PLS}(\omega) = \theta_{stack}(\omega)$. PLS is appropriate when trace amplitudes are comparable. However, the time-domain stack is amplitude weighted, so $\hat{\theta}_{PLS}(\omega)$ becomes biased whenever amplitude variability is present.

3.2 Phase masking via circular mean (PCM)

PCM addresses the amplitude bias inherent in PLS by removing amplitude information before the ensemble average is formed. Each spectrum is normalized to unit magnitude, ensuring all traces contribute with equal phase weight regardless of their spectral energy. The representative phase, for frequency ω and ensemble of n records is estimated using circular mean[11]

$$\hat{\theta}_{PCM}(\omega) = arg\left(\frac{1}{n}\sum_{k=1}^{n}\frac{A_k(\omega)}{|A_k(\omega)|}\right). \tag{7}$$

Since normalization precedes averaging, all traces contribute equally regardless of their spectral energy. $\hat{\theta}_{PCM}(\omega)$ is amplitude-invariant by construction. Circular mean provides a robust estimate of the dominant signal phase direction.[12] Importantly, Eq. (7) acts only on record phase; it does not modify the spectral magnitudes of the masked records themselves. The mask defined in Eqs. (4) and (5) is a unit-magnitude operator. Therefore, for every record, the spectral magnitude $|A_k(\omega)|$ and, consequently, the energy across n records, $(1/n)\sum |A_k(\omega)|^2$, is preserved. All changes induced by the mask arise solely from phase conditioning for both PLS and PCM.

The two estimators are nearly equivalent when amplitudes are comparable and increasingly differ as amplitude variability increases. PLS, therefore, has little amplitude bias when trace amplitudes are comparable but can bias the phase estimate toward higher-amplitude records otherwise. PCM eliminates this bias by construction, ensuring equal contribution from all traces regardless of spectral energy. The practical consequence is visible in Figs. 1(e)–1(h), which show the conditioned records under both idealized (uniform-amplitude) and realistic (variable-amplitude) conditions. Under

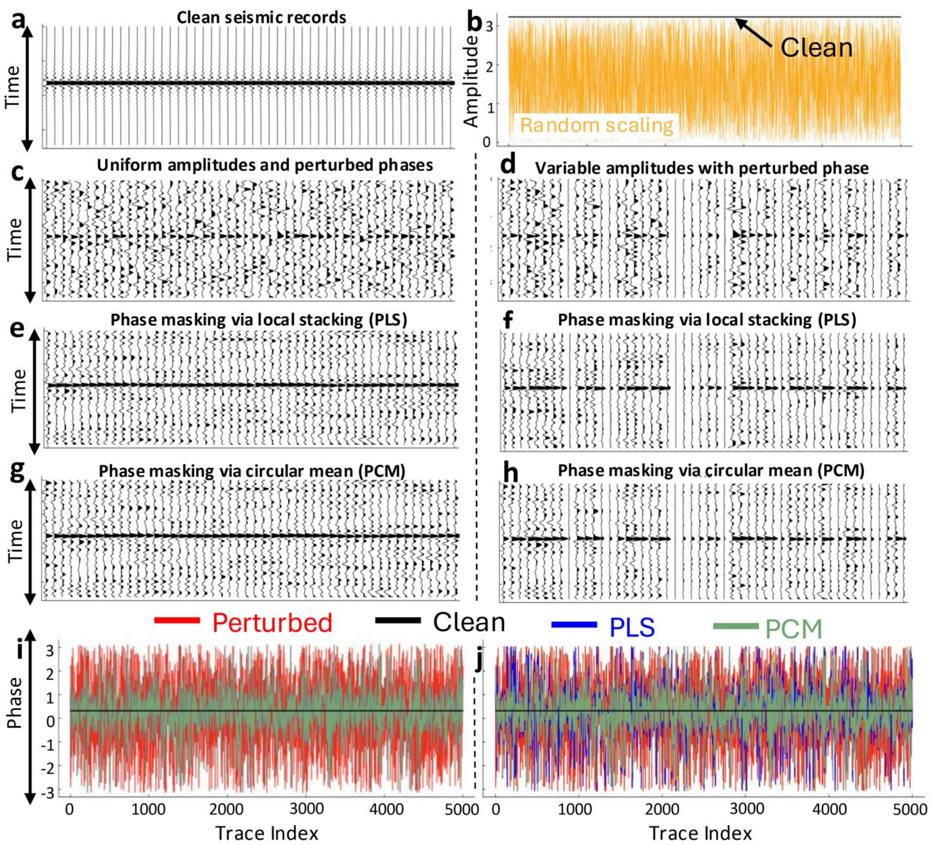

Fig. 1. Synthetic demonstration of phase masking under phase and amplitude perturbations. (a) Clean records with coherent phase and uniform amplitudes. (b) Record-dependent amplitude scalars drawn from a uniform distribution on [0, 1]. (c) Records with phase perturbations only. (d) Records with phase perturbations and amplitude scaling from (b). (e), (f) PLS applied to (c) and (d). (g), (h) PCM applied to (c) and (d). (i), (j) Wrapped phase across records at 5 Hz, before (i) and after (j) masking. Horizontal axis is trace index in all panels; every 100th trace is shown.

uniform amplitudes, PLS and PCM produce indistinguishable results [Figs. 1(e) and 1(g)], consistent with the theoretical equivalence in that limit. Under variable amplitudes, PCM yields noticeably more consistent phase alignment across the ensemble [Fig. 1(h)], while the PLS output shows larger residual phase scatter attributable to amplitude bias [Fig. 1(f)]. This divergence, absent under idealized conditions, becomes consequential in realistic acquisition scenarios and motivates the quantitative analysis in the Sec. 4.

4. Quantitative assessment of phase conditioning: PLS vs PCM

Having introduced both estimators, we now evaluate their performance under synthetic conditions using two measures: circular variance and signal-to-noise ratio (SNR).

The degree of phase coherence is quantified using circular variance,

$$V(\omega) = 1 - \left| \frac{1}{n} \sum_{k=1}^{n} \frac{A_k(\omega)}{|A_k(\omega)|} \right|, \tag{8}$$

which ranges from 0 (perfectly coherent) to 1 (perfectly uniform), providing an objective, amplitude-independent measure of phase dispersion across the ensemble.

SNR is estimated using semblance S as an intermediate variable,[13]

$$SNR_{dB} = 10\, log_{10} \frac{S}{1-S}, \tag{9}$$

where the semblance $\boldsymbol{S}$ is computed as

$$\mathrm{S} = \frac{\sum_{\boldsymbol{i}=1}^{\boldsymbol{N}} \left(\sum_{\boldsymbol{j}=1}^{\boldsymbol{M}} \boldsymbol{W}_{ij} \right)^2}{\boldsymbol{M} \sum_{\boldsymbol{i}=1}^{\boldsymbol{N}} \sum_{\boldsymbol{j}=1}^{\boldsymbol{M}} \boldsymbol{W}_{ij}^2}. \tag{10}$$

Here, N is the number of time samples in the analysis window, M is the number of records, and $\boldsymbol{W}_{\{ij\}}$ is the amplitude at time sample $\boldsymbol{i}$ on record $\boldsymbol{j}$.

We compare PLS and PCM under two scenarios designed to isolate the conditions under which the methods agree and where they differ: uniform amplitudes across records and variable amplitudes across records.

4.1 Case 1: Phase perturbations only with uniform amplitudes

Under uniform amplitudes, both PLS and PCM reduce phase variability equivalently, a result that confirms that the two estimators converge in the idealized limit. At 5 Hz, the perturbed ensemble of 5000 records exhibits a circular variance of V = 0.597 [Fig. 2(c)], indicating broad phase scatter around the dominant phase direction [Fig. 2(a)]. After applying either PLS or PCM, variance drops identically V = 0.268 [Figs. 2(d) and 2(e)], a 55% reduction, reflecting tighter

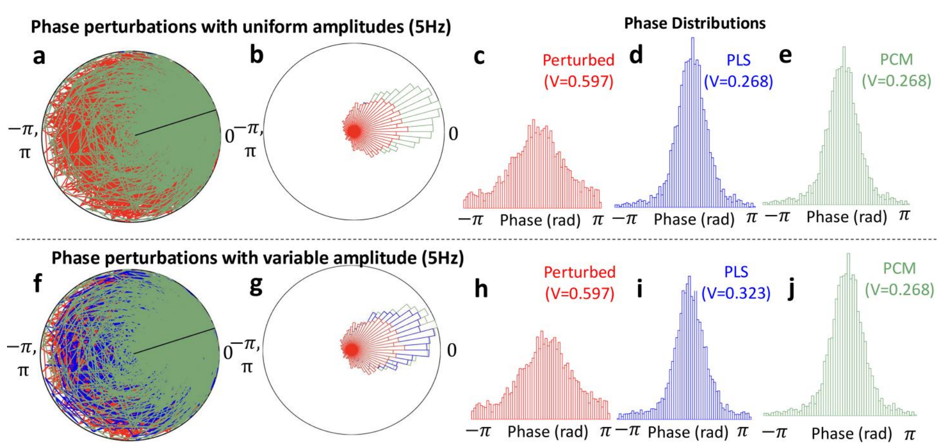

Fig. 2. Phase statistics illustrating phase masking performance at 5 Hz under phase perturbations with uniform amplitudes (top row) and with variable amplitudes (bottom row). (a), (f) Circular representation of phase ensembles across traces. (b), (g) Circular histograms of phase ensembles; red corresponds to perturbed data, blue to PLS, and green to PCM. (c), (h) Linear phase histograms of perturbed ensembles. (d), (i) Phase distributions after PLS. (e), (j) Phase distributions after PCM. Circular phase variance V is indicated in each panel. Under uniform amplitudes (top row), both masking approaches reduce phase variability similarly. When amplitudes vary (bottom row), PCM maintains consistently low variance, whereas PLS exhibits increased variance.

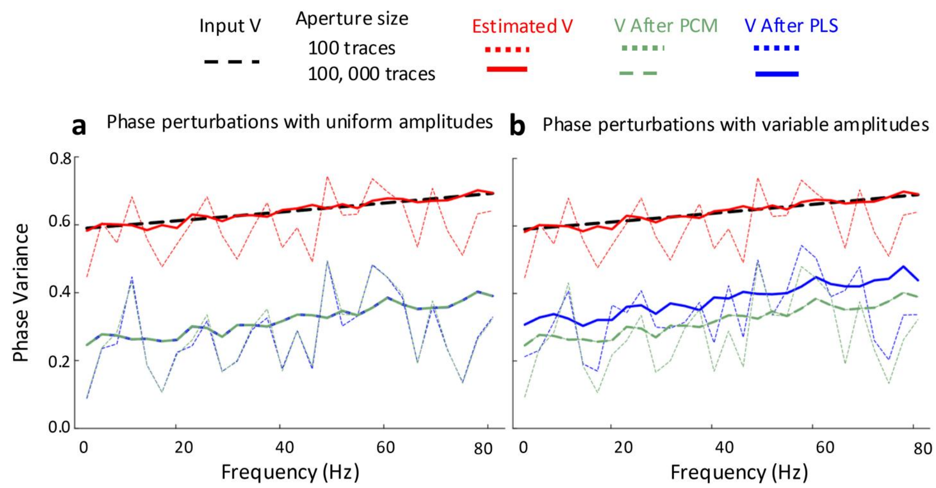

Fig. 3. Phase variance spectra for perturbed and phase-masked records. (a) Phase perturbations with uniform amplitudes. (b) Phase perturbations with additional trace-dependent amplitude variability. Red curves show phase variance of the perturbed data, blue curves correspond to PLS, and green curves to PCM. Dashed lines correspond to estimates from 100 seismic records and solid lines to estimates from 100 000 seismic records. In the phase-only case, both masking approaches reduce phase variance similarly. With amplitude variability, PCM maintains consistently lower variance than PLS across frequencies.

concentration of the phase distribution around the circular mean [Fig. 2(b), blue and green curves overlap]. Consistent with this, SNR improves from −8.09 to −0.55 dB after PLS and −0.56 dB after PCM. This equivalence holds across the full bandwidth [Fig. 3(a)].

When amplitudes are uniform, the time-domain stack provides an unbiased estimate of signal phase, making PLS a computationally simpler choice.

4.2 Case 2: Phase perturbations with variable amplitudes

Introducing record-dependent amplitude variability breaks the equivalence: PLS phase estimates become biased by amplitude mixing, whereas PCM remains robust by construction. This divergence is both statistically significant and physically consequential. At 5 Hz, after applying PLS, variance decreases only to $V = 0.32$ [Fig. 2(i)], a partial reduction of 45%, because the time-domain stack is dominated by high-amplitude records, pulling the representative phase away from the true signal phase. PCM eliminates this bias and reduces variance to $V = 0.26$ [Fig. 2(j)]. The circular representations in Figs. 2(f) and 2(g) make this contrast visually explicit: after PCM, phase clusters are as tight as in Case 1; after PLS, they remain substantially broader. Across the sull spectrum shown in Fig. 3(b), PCM maintains consistently lower phase variance than PLS. This is also reflected in SNR: starting from the same baseline of −9.14, PLS achieves −3.60 dB (a gain of 5.54 dB), while PCM reaches −2.52 dB (a gain of 6.62 dB).

These results are summarized in Table 1. Together, they establish that PLS and PCM are nearly equivalent when amplitudes are comparable. As amplitude variability increases, explicit amplitude-phase decoupling via circular-mean phase masking becomes increasingly important for reliable coherence conditioning.

5. Conclusions

We introduced an amplitude-invariant phase-masking framework for coherence conditioning in scattered wavefields. The key contribution is PCM, which estimates the dominant ensemble phase by normalizing spectra to unit magnitude prior to averaging, ensuring all records contribute with equal phase weight regardless of their spectral energy.

Table 1. Phase variance, semblance and SNR before and after phase masking using PLS and PCM, evaluated at 5 Hz for phase-perturbed records under uniform and scaled amplitude conditions.

		Phase variance (5 Hz)		Semblance		SNR (dB)	
Case	Method	Before	After	Before	After	Before	After
Uniform amplitudes	PLS	0.59	0.26	0.13	0.46	−8.09	−0.55
	PCM	0.59	0.26	0.13	0.46	−8.09	−0.56
Scaled amplitudes	PLS	0.59	0.32	0.10	0.30	−9.14	−3.60
	PCM	0.59	0.26	0.10	0.35	−9.14	−2.52

Circular statistics provides a natural language for characterizing ensemble phase: the circular mean identifies the dominant phase direction across multichannel records, while circular variance quantifies the spread around it. Unlike stacking-based approaches, which estimate a representative phase but provide no measure of phase dispersion, this framework captures both.

Controlled synthetic experiments show that PCM and the conventional PLS are equivalent when amplitudes are uniform. When strong trace-dependent amplitude variability is introduced, however, PLS becomes biased due to implicit amplitude weighting in the time-domain stack. PCM avoids this bias and consistently achieves lower phase variance across the bandwidth, producing more coherent summation.

These results demonstrate that amplitude-phase decoupling is helpful for reliable coherence conditioning in realistic multichannel data. Because the proposed formulation integrates directly with existing masking workflows, it provides a practical path toward improved phase stabilization and more robust coherence recovery in seismic imaging and other wave-based sensing applications.

Author Declarations

Conflict of Interest

The authors have no conflicts to disclose.

Data Availability

The code and data reproducing all results are available on Zenodo.[14] The data that support the findings of this study are openly available in GitHub at https://github.com/arohatgi29/SeismicPhaseStatistics/tree/main/Rohatgi-et-al-2026-JASA.

References

[1] A. V. Oppenheim and J. S. Lim, "The importance of phase in signals," Proc. IEEE **69**, 529–541 (1981).
[2] H. L. Van Trees, *Optimum Array Processing: Part IV of Detection, Estimation, and Modulation Theory* (Wiley, New York, 2002).
[3] K. Paliwal, K. Wójcicki, and B. Shannon, "The importance of phase in speech enhancement," Speech Commun. **53**, 465–494 (2011).
[4] D. S. Williamson, Y. Wang, and D. Wang, "Complex ratio masking for monaural speech separation," IEEE/ACM Trans. Audio. Speech. Lang. Process. **24**, 483–492 (2016).
[5] R. M. Goldstein and C. L. Werner, "Radar interferogram filtering for geophysical applications," Geophys. Res. Lett. **25**, 4035–4038, https://doi.org/10.1029/1998GL900033 (1998).
[6] A. Bakulin, I. Silvestrov, and D. Neklyudov, "Importance of phase guides from beamformed data for processing multi-channel data in highly scattering media," J. Acoust. Soc. Am. **147**, EL447–EL452 (2020).
[7] A. Bakulin, D. Neklyudov, and I. Silvestrov, "Seismic time-frequency masking for suppression of seismic speckle noise," Geophysics **88**, V371–V385 (2023).
[8] J. W. Goodman, *Speckle Phenomena in Optics: Theory and Applications* (Roberts and Company, Englewood, CO, 2007).
[9] A. Bakulin, D. Neklyudov, and I. Silvestrov, "Multiplicative random seismic noise caused by small-scale near-surface scattering and its transformation during stacking," Geophysics **87**, V419–V435 (2022).
[10] A. V. Oppenheim, R. W. Schafer, and J. R. Buck, *Discrete-Time Signal Processing*, 2nd ed. (Prentice Hall, Upper Saddle River, NJ, 1999).
[11] K. V. Mardia and P. E. Jupp, *Directional Statistics* (Wiley, New York, 2009).
[12] A. Rohatgi, A. Bakulin, and S. Fomel, "Data-driven analysis of seismic phase using circular statistics," Leading Edge **44**, 683–691 (2025).
[13] A. Bakulin, I. Silvestrov, and M. Protasov, "Signal-to-noise ratio computation for challenging land single-sensor seismic data," Geophys. Prospect. **70**, 629–638 (2022).
[14] A. Rohatgi, A. Bakulin, and S. Fomel, "Code and data for 'Amplitude-invariant phase masking for coherence recovery in scattered wavefields' (version 1.0.0) [software]," https://zenodo.org/records/20059964 (Last viewed June 19, 2026).